

From Point Clouds to Cultural Landscapes: Open-Source Machine Learning Applications for Archaeological UAV LiDAR segmentation

Nicodemo Abate¹, Alessia Frisetti¹, Gabriele Ciccone¹, Antonio Minervino Amodio¹, Maria Sileo¹,
Rosa Lasaponara², Nicola Masini¹

¹ National Research Council – Institute of Heritage Science, Cd. S. Loja, 85050, Tito Scalo (PZ),
Italy, nicodemo.abate@cnr.it, alessia.frisetti@cnr.it, gabriele.ciccone@cnr.it,
antonio.minervinoamodio@cnr.it, maria.sileo@cnr.it, masini.nicola@cnr.it,

² National Research Council – The Institute of Methodologies for Environmental Analysis, Cd. S.
Loja, 85050, Tito Scalo (PZ), rosa.lasaponara@cnr.it

Abstract – This study presents an open-source methodological workflow for processing Unmanned Aerial System (UAS) LiDAR data using a probabilistic machine learning algorithm to enhance the visibility and detection of archaeological features under vegetation. The proposed framework combines the 3DMASC plugin for CloudCompare with the Relief Visualization Toolbox (RVT) and QGIS to deliver an accessible, non-programmer-friendly solution for point cloud classification and derivative model enhancement. The methodology is validated through two case studies: the Kastro-Pandosia site in Epirus, Greece, and Torre Castiglione in Apulia, Italy. Both sites, obscured by dense vegetation, revealed critical archaeological structures—including defensive walls, terraces, and ancient routes—following segmentation and visualization. Results confirm the robustness and replicability of the approach, reinforcing the value of open-source strategies in archaeological remote sensing.

I. INTRODUCTION

In the 21st century, archaeological research has undergone a profound transformation due to the widespread adoption of advanced remote sensing technologies. Among these, two innovations have been particularly influential: Light Detection and Ranging (LiDAR) systems and Unmanned Aerial Systems (UASs). Together, these technologies have redefined the scope and methods of archaeological fieldwork, particularly in environments where traditional techniques are hindered by dense vegetation, topographic complexity, or restricted accessibility [1].

LiDAR systems, as active remote sensing instruments, provide high-resolution three-dimensional data capable of penetrating vegetative cover and capturing microtopographic variations with centimetric or even

millimetric precision. When deployed on aerial platforms such as UAVs, these sensors offer a cost-effective and versatile alternative to traditional manned flights, significantly reducing operational costs and logistical constraints. This synergy has enabled researchers to detect, document, and interpret archaeological features previously hidden beneath forest canopies or located in areas difficult to access using conventional methods. The growing availability of UAS-mounted LiDAR systems has coincided with an increasing need for efficient, accessible, and reproducible processing workflows. While commercial software packages provide powerful analytical capabilities, their prohibitive costs and steep learning curves often limit their adoption, particularly among institutions with constrained resources or researchers without programming expertise. Moreover, the core analytical challenge—namely, the classification and segmentation of LiDAR point clouds—remains a critical bottleneck in archaeological applications [2,3].

To address these limitations, recent research has focused on developing open-source, user-friendly methodologies that allow for advanced processing without requiring deep technical skills. In particular, the integration of machine learning techniques, such as Random Forest classification, into open-source platforms like CloudCompare (with the 3DMASC plugin) has provided a powerful alternative. These tools enable the segmentation of complex LiDAR datasets based on geometric and spectral attributes, supporting the generation of refined digital models—Digital Terrain Models (DTMs), Digital Surface Models (DSMs), and Digital Feature Models (DFMs)—essential for archaeological interpretation [4–8].

At the same time, the application of advanced visualization tools, such as the Relief Visualization Toolbox (RVT) [9], has enhanced the interpretability of LiDAR-derived products. By employing multiple derivative raster layers (e.g., hillshade, slope, SLRM, MSRM), RVT enhances the visibility of subtle topographic

anomalies and structural patterns. When combined with GIS environments like QGIS, these enhanced outputs support integrative spatial analyses that link remote sensing results with archaeological, historical, and environmental datasets.

This paper presents a unified open-source methodological framework for the processing and interpretation of UAS LiDAR data in archaeological contexts, structured around a probabilistic machine learning approach. We demonstrate the utility and replicability of this approach through two case studies located in southern Europe, each characterized by dense vegetation and a complex archaeological landscape: (i) the Hellenistic-Byzantine fortified settlement of Kastri-Pandosia in Epirus (Greece) [10], and (ii) the medieval rural site of Torre Castiglione in Apulia (Italy) [11]. Despite their geographical and historical differences, both sites present similar methodological challenges that make them ideal for testing and validating a shared processing pipeline.

In both cases, the integration of 3DMASC-based Random Forest classification, RVT-derived enhancements, and GIS-based interpretation allowed for the effective extraction of archaeological features otherwise obscured by vegetation and topography. The approach enabled the identification of defensive walls, terraces, buildings, paths, and other anthropogenic features, often invisible in traditional aerial imagery or satellite data. Through these examples, we aim to showcase how the proposed workflow can serve as a practical and scalable solution for archaeological prospection and documentation, especially in under-canopy or remote sites.

By prioritizing accessibility, replicability, and technical robustness, the presented methodology contributes to the democratization of high-resolution landscape archaeology. It facilitates the use of cutting-edge tools by a wider community of archaeologists, cultural heritage professionals, and territorial planners, fostering a more inclusive and technologically empowered approach to heritage research.

This research was funded by (i) PANDOSIA project, winner of the European Call 2023 for access to the E-RIHS mobile laboratories for the LiDAR data acquisition and processing, and (ii) CHANGES project (National Recovery and Resilience Plan, Mission 4, Component 2, Investment Line 1.3 ‘Extended Partnerships’), Spoke 5, WP3 and Spoke 7, for the post-processing and machine learning-based application.

II. CASE STUDIES

The proposed open-source machine learning-based workflow was validated through two case studies: the Hellenistic-Byzantine fortified site of Kastri-Pandosia in Epirus (Greece) and the medieval settlement of Torre Castiglione in Apulia (Italy). Despite their

geomorphological and chronological differences, both sites present similar challenges—namely, dense Mediterranean vegetation, irregular terrain morphology, and incomplete archaeological records. These conditions make them ideal benchmarks to test the robustness, adaptability, and scalability of the methodological framework.

A. Kastri-Pandosia (Epirus, Greece)

Kastri-Pandosia is situated in a mountainous and forested region of northwestern Greece, along the Acheron River valley. The site comprises a fortified settlement founded in the 3rd century BCE by the Molossian dynasty and reused in the medieval period. Extensive vegetation, combined with terrain roughness and limited accessibility, has historically impeded archaeological investigations.

B. Torre Castiglione (Apulia, Italy)

Located in the karstic plateau of the Murge near Conversano (Bari), Torre Castiglione is a rural fortified settlement occupied from the Iron Age through the late Middle Ages. Its most prominent visible feature is a 15-meter-high watchtower dating to the Angevin period, but the surrounding remains are mostly obscured by dense Mediterranean scrub and abandoned agricultural terraces.

III. METHODS

The core of the approach consists of three primary steps (Table 1): (i) Point Cloud Generation and Cleaning: UAS-based LiDAR survey and outlier removal; (ii) Probabilistic Machine Learning Classification: Segmentation via Random Forest in CloudCompare 3DMASC; (iii) Raster Derivative Creation and Enhancement: Generation of DSM, DTM, DFM followed by RVT-based enhancements and GIS integration (Fig. 1).

Table 1. Description of the flowchart.

Component	Tool/Software	Description
Point cloud acquisition	UAS + Riegl MiniVux-3 LiDAR	Drone-mounted 5-echo TOF LiDAR
Pre-processing	CloudCompare v2.14	Noise filter, SOR, spatial resampling (0.1 m spacing)
Classification	CloudCompare + 3DMASC	Random Forest (250 trees, depth 25, leaf size 10)
Feature enhancement	RVT v2.2.1	SLRM, MSRM, MSTP, hillshade, slope, PCA
Mapping	QGIS (v3.28 or higher)	Layer integration and archaeological map production

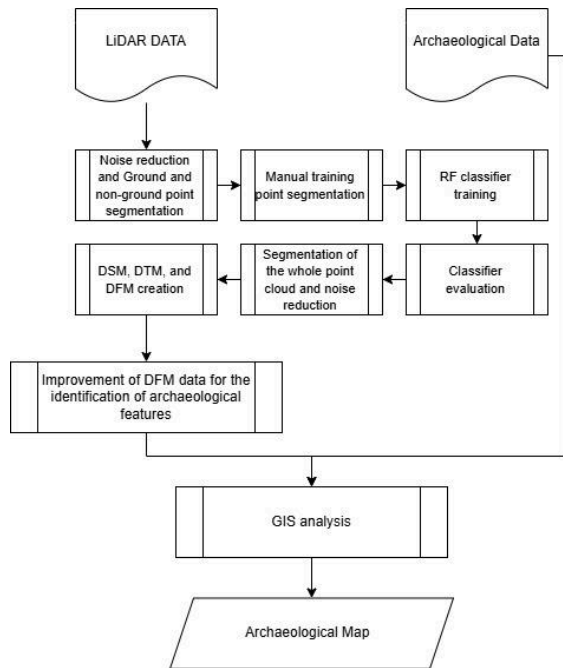


Fig. 1. Operational Flowchart.

The segmentation and classification of LiDAR-derived point clouds represent a critical step in transforming raw 3D data into actionable archaeological information. In the proposed methodology, this process is implemented through a fully open-source workflow, leveraging the 3DMASC plugin within CloudCompare and a Random Forest (RF) machine learning algorithm to achieve accurate and interpretable results without the need for proprietary software or advanced programming skills.

The methodological framework follows a structured sequence of operations, which includes: (i) Point cloud cleaning and preprocessing; (ii) Training sample creation and manual labelling; (iii) Feature computation and multi-scale analysis; (iv) Classifier training and hyperparameter tuning; (v) Classification of the full dataset; (vi) Extraction of raster models (DTM, DSM, DFM).

Each step was designed to maximize interpretability and reproducibility while ensuring robustness against site-specific challenges such as irregular topography, high vegetation density, and partial occlusion of features.

Once the LiDAR survey data were acquired and the georeferenced point cloud generated, the first step consisted of data cleaning to remove noise and outliers. Two filters were applied within CloudCompare: (i) Noise Filter: This tool fits a local plane to each point and removes those whose distance from the plane exceeds a defined threshold, effectively functioning as a low-pass spatial filter; (ii) Statistical Outlier Removal (SOR): This method computes the average distance of each point from its k -nearest neighbors and eliminates those significantly deviating from the mean. For both case studies, parameters

were set at $k = 8$ and $\sigma = 2$.

Subsequently, the cleaned point cloud was resampled to ensure spatial homogeneity, using a minimum point spacing of 0.1 m. This resampling step reduces data redundancy and improves computational efficiency without significantly compromising spatial detail.

A. Training Sample Selection and Manual Labelling

The Random Forest [12] classifier used in 3DMASC requires a supervised training dataset. Representative samples were manually segmented and labeled within CloudCompare using the Interactive Segmentation Tool. The classification scheme was based on simplified ASPRS categories, tailored for archaeological relevance: (i) Ground; (ii) Low vegetation; (iii) High vegetation; (iv) Built structures (archaeological or modern).

Training samples were selected to cover diverse scenarios across the survey area, ensuring representative variation in both geometric and radiometric attributes. Approximately 70% of the samples were used for training and 30% for testing, allowing internal performance validation before full-scale application.

B. Multi-Attribute, Multi-Scale Feature Computation

The 3DMASC plugin supports the extraction of a wide range of geometric, structural, and spectral features from the point cloud, computed at multiple neighborhood radii. In both studies, features were calculated at the following radii (sphere diameter): 0.2, 0.4, 0.6, 0.8, 1.0, 1.2, 1.4, and 1.6 m, to capture variation across fine to coarse spatial scales. These features are sensitive to local geometric variations and have demonstrated strong discriminative power in previous LiDAR classification studies in archaeology [13].

C. Random Forest Classification and Hyperparameter Tuning

The Random Forest algorithm was selected due to its robustness, low overfitting tendency, and interpretability. The classification was performed using 3DMASC's embedded RF engine with an iterative tuning of three key hyperparameters: (i) Number of trees: tested from 5 to 250; (ii) Maximum tree depth: 25 and 50; (iii) Minimum sample count (leaf size): 10 and 20.

Each configuration was evaluated using standard performance metrics—Precision, Recall, F1-score, and Overall Accuracy—on the testing subset.

D. Application to Full Dataset and Raster Generation

Once the classifier was finalized, it was applied to the full point cloud. Misclassified or low-confidence points were filtered out using built-in confidence thresholds and SOR. The final classified cloud was split into ground and off-ground components, enabling the generation of: (i) Digital Terrain Model (DTM): bare-earth model excluding vegetation and structures; (ii) Digital Surface Model

(DSM): includes all surface elements; (iii) Digital Feature Model (DFM): focuses on anthropogenic and archaeological structures.

Raster models were exported at 0.2 m/pixel resolution, suitable for feature enhancement and integration into GIS platforms.

IV. RESULTS

A. Classification Performance and Segmentation Outcomes

The implementation of the proposed open-source machine learning workflow yielded consistent and robust classification results across both case studies, despite variations in point cloud density, vegetation cover, and archaeological context.

For the Kastri-Pandosia dataset (average density: ~2000 points/m²), the Random Forest classifier trained via the 3DMASC plugin demonstrated high performance. Among the ten tested configurations, the best results were obtained using 250 decision trees, a maximum tree depth of 25, and a minimum sample count of 10. This configuration reached an overall accuracy of 85.03%, with precision and recall values exceeding 0.84 for the key classes of interest: ground, high vegetation, low vegetation, and buildings. The classification matrix indicated balanced performance across classes, with minimal confusion between vegetation strata and built structures—an essential requirement for accurate Digital Feature Model (DFM) generation.

At Torre Castiglione, the average point density was lower (~850 points/m²), yet the same classifier parameters yielded comparable results. Here, the overall classification accuracy was 84.71%, with particularly strong performance in distinguishing ground from vegetation. Despite the presence of irregular canopy cover and degraded structural remains, the model successfully segmented out archaeological features such as masonry walls, terraces, and partially buried architectural units. The slightly reduced precision in classifying high vegetation, compared to Kastri, was attributed to more heterogeneous vegetative compositions and lower point cloud density, but did not significantly affect the reliability of structural identification.

In both sites, the training process required approximately 6 to 8 hours, depending on dataset size and feature computation complexity. Feature importance analysis consistently ranked the following variables among the most influential in the classification process: planarity (PLANA), sphericity (SPHER), dip angle (NORMDIP), PCA components, and return number (RETNB). These features proved particularly effective at differentiating anthropogenic surfaces from irregular vegetated terrain, especially when computed at multiple radii (from 0.8 to 1.6 m).

B. Archaeological Observations

Although the focus of this study lies in the processing

methodology, both case studies confirmed the archaeological value of the outputs. At Kastri-Pandosia, the enhanced DFM revealed the full perimeter of the ancient fortified wall, terracing aligned with the topography, and probable access paths that had not been previously mapped. At Torre Castiglione, the segmentation and RVT enhancement allowed for the identification of at least 44 topographic units, including burial structures, habitation zones, and hydraulic features, many of which were previously undocumented due to dense vegetation.

In both cases, the integration of machine learning-based classification and visual enhancement led to the refinement of existing site maps and facilitated the recognition of subtle anthropogenic modifications to the landscape—demonstrating the interpretive power of the methodology when applied systematically and with archaeological awareness (Fig. 2).

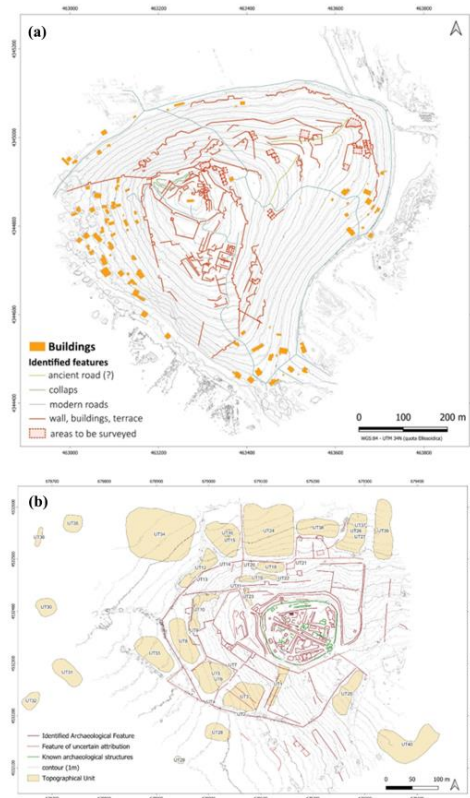


Fig. 2. Archaeological results obtained from the analysis of LiDAR data derived: (a) Kastri, (b) Torre di Castiglione.

V. CONCLUSION

This study demonstrates the efficacy and replicability of an open-source, machine learning-based methodology for processing LiDAR data acquired from unmanned aerial systems (UAS) in archaeological contexts. By integrating

probabilistic classification techniques through the 3DMASC plugin in CloudCompare, with high-resolution raster enhancement via the Relief Visualization Toolbox (RVT), we developed and tested a complete, user-friendly workflow that allows for the segmentation, visualization, and interpretation of complex landscape features—even in highly vegetated and topographically irregular environments.

The application of this workflow to two distinct case studies—Kastri-Pandosia in Greece and Torre Castiglione in Italy—has demonstrated its flexibility and robustness across different archaeological scenarios. In both contexts, the Random Forest classifier achieved an overall accuracy exceeding 84%, reliably distinguishing ground surfaces, vegetation types, and built structures within dense point clouds of varying resolutions. This consistency confirms the adaptability of the method to site-specific conditions without compromising classification performance.

From a technical perspective, the approach provides several key advantages, such as: (i) accessibility; (ii) interpretability; (iii) scalability; (iv) integration.

While the archaeological results presented were summarized, both case studies underscore the practical value of the method in revealing features that are typically inaccessible through traditional survey techniques. The identification of defensive walls, terraces, routes, tombs, and architectural fragments illustrates the potential of LiDAR combined with machine learning not merely as a mapping tool, but as an active instrument of discovery and interpretation.

Importantly, this workflow addresses a current gap in archaeological remote sensing: the need for tools that are not only powerful and precise but also transparent, shareable, and adaptable to diverse user needs. By privileging open technologies and reproducible methods, it aligns with broader movements in digital archaeology that emphasize open science, data democratization, and methodological transparency.

REFERENCES

- [1] S.Crutchley, “The Light Fantastic – Using Airborne Lidar in Archaeological Survey”, 2010;38.
- [2] E.Lozić, B.Štular, “Documentation of Archaeology-Specific Workflow for Airborne LiDAR Data Processing”, *Geosciences*, 2021, vol.11, (No.1):26. <https://doi.org/10.3390/geosciences11010026>.
- [3] B. Štular, E.Lozić, “2Comparison of Filters for Archaeology-Specific Ground Extraction from Airborne LiDAR Point Clouds”, *Remote Sens.*, 2020; vol.12:3025. <https://doi.org/10.3390/rs12183025>.
- [4] M.Letard, D.Lague, A.Le Guennec, S.Lefèvre, B.Feldmann, P.Leroy, et al. “3DMASC: Accessible, explainable 3D point clouds classification. Application to BI-spectral TOPO-bathymetric lidar data ISPRS J Photogramm”, *Remote Sens.*, 2024; vol.207, pp.175–197. <https://doi.org/10.1016/j.isprsjprs.2023.11.022>.
- [5] B.Suleymanoglu, M.Soycan, “Comparison of filtering algorithms used for DTM production from airborne lidar data: a case study in Bergama, Turkey”, *Geod Vestn*, 2019; vol.63, pp.395–414. <https://doi.org/10.15292/geodetski-vestnik.2019.03.395-414>.
- [6] O.Bollandsås, O.Risbøl, L.Ene, A.Nesbakk, T.Gobakken, E.Næsset, “Using airborne small-footprint laser scanner data for detection of cultural remains in forests: An experimental study of the effects of pulse density and DTM smoothing” *J. Archaeol. Sci.*, 2012; vol.39:2733–43. <https://doi.org/10.1016/j.jas.2012.04.026>.
- [7] N.Masini, N.Abate, F.T.Gizzi, V.Vitale, A.Minervino Amodio, M.Sileo, et al., “UAV LiDAR Based Approach for the Detection and Interpretation of Archaeological Micro Topography under Canopy—The Rediscovery of Peticara (Basilicata, Italy)”, *Remote Sens.*, 2022; vol.14:6074. <https://doi.org/10.3390/rs14236074>.
- [8] M.Danese, D.Gioia, V.Vitale, N.Abate, A.Minervino Amodio, R.Lasaponara et al., “Pattern Recognition Approach and LiDAR for the Analysis and Mapping of Archaeological Looting: Application to an Etruscan Site”, *Remote Sens.*, 2022; vol.14, No.7:1587. <https://doi.org/10.3390/rs14071587>.
- [9] Ž.Kokalj, K.Zakšek, K.Oštir P.Pehani, K.Čotar, M.Somrak, “Relief Visualization Toolbox, ver. 2.2.1”, Manual, 2020:11.
- [10] N.Abate, D.Roubis, A.Aggeli, M.Sileo, A.Minervino Amodio, V.Vitale et al., “An Open-Source Machine Learning-Based Methodological Approach for Processing High-Resolution UAS LiDAR Data in Archaeological Contexts: A Case Study from Epirus, Greece”, *J. Archaeol. Method. Theory*, 2025; vol.32:38. <https://doi.org/10.1007/s10816-025-09706-8>.
- [11] N.Abate, R.Goffredo, G.Dato, A.Minervino Amodio, A.Loperte, A.Frisetti et al., “Adopting an Open-Source Processing Strategy for LiDAR Drone Data Analysis in Under-Canopy Archaeological Sites: A Case Study of Torre Castiglione (Apulia)”, *Remote Sens.*, 2025; vol.17:1134. <https://doi.org/10.3390/rs17071134>.
- [12] L.Breiman, “Random Forests”, *Mach. Learn.* 2001; vol.45, pp.5–32. <https://doi.org/10.1023/A:1010933404324>.